Proceeding of the IEEE
International Conference on Robotics and Biomimetics
Dali, China, December 2019

Design and Analysis of a Novel Deployable Robotic Grasper

Changqing Gao
Department of Mechanical Engineering and Automation
Harbin Institute of Technology (Shenzhen)
Shenzhen 518055, China
18B953058@stu.hit.edu.cn

Hailin Huang and Bing Li*
Department of Mechanical Engineering and Automation
Harbin Institute of Technology (Shenzhen)
Shenzhen, Guangdong Province, China
{Huanghailin & libing.sgs}@hit.edu.cn

***Abstract* - In order to grasp large-scale unknown objects, a novel deployable robotic grasper is presented in this paper, which is composed of a train of basic metamorphic mechanism modules. Firstly, a detailed mechanism design is introduced, in which a scissor-shaped mechanism is used to design basic module so that it has single deployment mobility and a particular metamorphic mechanism is applied to change its mobility from deployment motion to grasping motion. Then, metamorphic process, mobility analysis, and singularity analysis of the basic module are conducted and the assembling of the grasper is illustrated. Secondary, the deploy/fold ratio and its influencing factors are discussed. Thirdly, the workspace of the grasper is demonstrated, which shows that the grasper has large reachable workspace. In addition, kinematic equation and dexterity of the proposed grasper are also presented. Finally, the shape adaptability and grasping simulation are conducted, which shows that the grasper has good grasping performances and can be used to grasp large-scale unknown objects.**

Index Terms* - *Deployable robotic grasper, Metamorphic mechanism, Deploy/fold ratio, Shape adaptability.

I. INTRODUCTION

Currently, robotic grasping has become a hot research topic, which has aroused the interests of a large of researchers. [1]. At present, those proposed grasping schemes previously can be mainly divided into serial mechanisms, parallel mechanisms, and serial-parallel mechanisms. Serial mechanisms usually achieve better results in grasping lightweight objects due to its small stiffness [2]. Compared with serial mechanisms, parallel mechanisms have complementary merits in the robotic graspers, the advantages of which include higher stiffness, lower inertia, and a higher carrying capacity. However, the traditional parallel mechanisms always have very limited workspace [3]. In order to utilize their advantages and avoid their disadvantages, serial-parallel mechanisms were designed, which usually is assembled via connecting a train of parallel modules in series [4]. Obviously, serial-parallel mechanisms not only have great stiffness but also have large reachable workspace by controlling the number of parallel modules.

However, series-parallel mechanisms have not been used too much in the design of robotic grasper, the main reason of which includes two factors. On the one hand, traditional series-parallel mechanisms cannot be deployed. So it cannot be conveniently transported and stored [5] [6] [7] [8] [9]. Inspired by such challenge, Li proposed a novel grasping manipulator for grasping large-scale unknown objects [10]. On the other hand, the end-effectors of serial-parallel mechanisms are not suitable for grasping tasks while serial-parallel mechanisms always have so many actuators. So how to achieve more motions with fewer actuators become a key point. Numerous studies have shown that metamorphic mechanism will be a nice answer out of the dilemma [11] [12]. A large number of researchers have applied metamorphic mechanism into their own design [13].

Based on above analysis, due to various disadvantages such as small workspace, small stiffness, and large volume of those graspers proposed previously, so it is difficult to apply them into grasping large-scale unknown objects. Therefore, a type of robotic grasper, which can be used to grasp large-scale unknown objects, needs to be designed. Such type of robotic grasper is required the following features:

1. The robotic grasper needs good stiffness to grasp large mass objects, so truss-shaped structure must be adopted in design.
2. A good deploy/fold ratio is necessary for convenient of storage and transportation.
3. Robotic grasper is required good shape adaptability for grasping unknown objects.
4. Lightweight is essential for grasping objects, under-actuated grasper is a good method to solve such a problem.

This paper presents a novel deployable robotic gasper, which is composed of five basic deployable metamorphic mechanism modules. In each module, scissor-shaped mechanism is used to perform deployment motion. Especially kinematic metamorphic mechanism is adopted to change mobility from deployment motion to grasping motion. To ensure grasping stiffness of the robotic grasper, truss-shaped structure is applied into the design of the module. Then, the analysis of deploy/fold ratio, workspace, dexterity, and shape adaptability proves that the proposed gasper has excellent grasping performances. The rests of this paper are organized as follows. In the next section, a detailed mechanism design is introduced. Then, metamorphic process, mobility analysis, and singularity analysis of the basic module are presented and the assembling of the grasper is illustrated. In Section 3, the deploy/fold ratio and its influencing factors of the robotic grasper are discussed. In section 4, dexterity and workspace of the grasper are proposed. Section 5 discusses shape adaptability and grasping simulation for different-shaped objects. Section 6 concludes this paper.

978-1-7281-6321-5/19//$31.00 ©2019 IEEE

II. Design of Deployable Robotic Grasper

A. *Design of the Metamorphic Module*

Basic metamorphic mechanism module is made up of three parts including deployable mechanism, metamorphic mechanism, and supporting mechanism.

In order to realize the deployment motion, scissor-shaped mechanism is used into module design as shown in Fig. 1. Link 6 and link 7 are connected by revolute joint R_{13}, then the scissor-shaped mechanism is connected with upper metamorphic mechanism by revolute joints R_5, R_6 and lower metamorphic mechanism by revolute joints R_7, R_8. The two metamorphic mechanisms and the scissor-shaped mechanism constitute the grasping sub-mechanism, which will directly contact with different-shaped objects.

In supporting mechanism, link 8 is rigidly connected with link 9 and upper metamorphic mechanism. Similarly, link15 is rigidly connected with link 14 and lower metamorphic mechanism. Then, link 10 is connected with link 9 by revolute joint R_{11} and link 11 by prismatic joint P_5, link 11 is connected with link 12 by revolute joint R_{10} and lower metamorphic mechanism by revolute joint R_9. Finally, link 13 is connected with link 15 by prismatic joint P_6 and link 12 by revolute joint R_{12}.

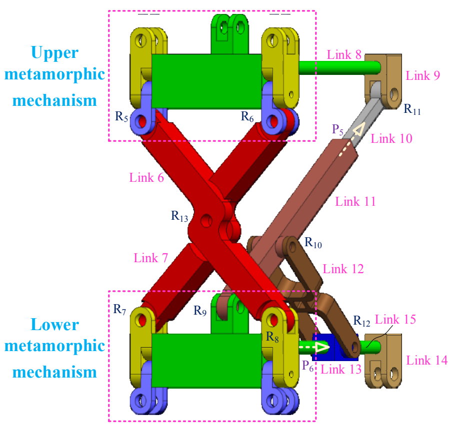

Fig. 1 Basic metamorphic mechanism module.

Metamorphic mechanism is as shown in Fig. 2, which is composed of five links. Link 1 is connected with link 3 by revolute joint R_1 and link 5 by prismatic joint P_1. Similarly, link 2 is connected with link 4 by revolute joint R_2 and link 5 by prismatic joint P_2. When the module performs the deployment motion, the scissor-shaped mechanism is in operation. Due to special structure designs of link 3, link4, and link 5 are as shown in partial view A of Fig. 2, link 3 and link 5 actually form prismatic joint P_3, link 4 and link 5 form prismatic joint P_4. In such process, the upper metamorphic mechanism relate to the lower metamorphic mechanism have a translational mobility, the scissor-shaped mechanism is equivalent to prismatic joint P in the side view of module as shown in Fig. 3(a). Based on the modified Grübler–Kutzbach mobility criterion, the mobility of deployment motion can be calculated as:

$$M = d\left(n-g-1\right)+\sum_{i=1}^{g} f_i + v - \xi = 3(6-7-1)+7+0+0=1 \quad (1)$$

where d is the rank of the mechanism, the rank of the planar mechanism is 3; n is the number of links, which is 6 in this module; g is the number of joints, which is 7 in this module; f_i is the degree of freedom for the i joint; v is the number of redundant constrains, which is 0 in this module; ξ is the number of local mobility, which is 0 in this module.

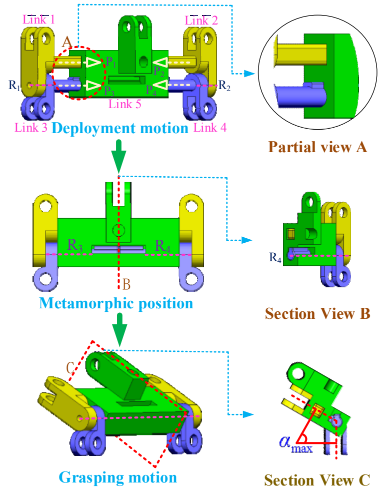

Fig. 2 Metamorphic process of the metamorphic mechanism.

When module is deployed in metamorphic position, it is obvious that physical limit is designed to ensure the module can be only deployed in this configuration as shown in section view B of Fig. 2. No doubt that the link1, link 2, and link 5 can be rotated around the axes of R_1 and R_2, such process is called grasping motion. At present, link 3 and link 5 actually form the revolute joint R_3, link 4 and link 5 actually form the revolute joint R_4. Link 5 relate link 3 and link 4 have one revolute mobility R in the side view of module as shown in Fig. 3(b).

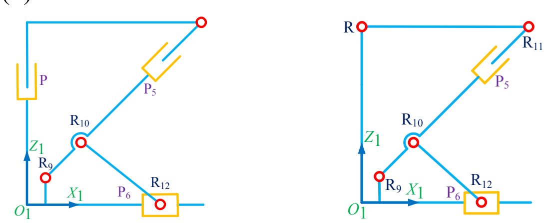

(a) Deployment motion process. (b) Grasping motion process.

Fig. 3 Metamorphic motion of the module.

In the grasping motion process, based on the modified Grübler–Kutzbach mobility criterion, the mobility of grasping motion can be calculated as:

$$M = 3\left(6-7-1\right)+7=1 \quad (2)$$

Based on the aforementioned analysis, metamorphic mechanism module has one degree of freedom in both deployment motion process and grasping motion process. So only one actuator is needed to perform two motions, which is of great significance to the lightweight of the grasper. Besides, special structure design ensures that the basic module has definite maximum grasping angle, $\alpha_{\max}$, as shown in section view C of Fig. 2. Such design of maximum grasping angle has important impact on the size of the module.

In addition to mobility analysis, singular analysis is also important because it determines whether the grasper can successfully complete the deployment motion and grasping motion. A coordinate frame $\{O_1\text{-}X_1Y_1Z_1\}$ is established with Z_1-axis along the translational direction of the prismatic pair P, X_1-axis along the translational direction of the prismatic pair P_6, Y_1-axis is determined by the right-hand rule, as shown in Fig. 3. Then, the twist system of deployment motion in the side view of module can be given as

$$\begin{cases} \boldsymbol{S}_{\mathrm{p}} = (0,\ 0,\ 0;\ 0,\ 0,\ 1) \\ \boldsymbol{S}_{\mathrm{P}_5} = (0,\ 0,\ 0;\ d_{\mathrm{P}_5},\ 0,\ f_{\mathrm{P}_5}) \\ \boldsymbol{S}_{\mathrm{P}_6} = (0,\ 0,\ 0;\ 1,\ 0,\ 0) \\ \boldsymbol{S}_{\mathrm{R}_9} = (0,\ 1,\ 0;\ d_{\mathrm{R}_9},\ 0,\ f_{\mathrm{R}_9}) \\ \boldsymbol{S}_{\mathrm{R}_{10}} = (0,\ 1,\ 0;\ d_{\mathrm{R}_{10}},\ 0,\ f_{\mathrm{R}_{10}}) \\ \boldsymbol{S}_{\mathrm{R}_{11}} = (0,\ 1,\ 0;\ d_{\mathrm{R}_{11}},\ 0,\ f_{\mathrm{R}_{11}}) \\ \boldsymbol{S}_{\mathrm{R}_{12}} = (0,\ 1,\ 0;\ d_{\mathrm{R}_{12}},\ 0,\ f_{\mathrm{R}_{12}}) \end{cases} \tag{3}$$

Obviously, the rank of the twist system is 3 and the twist system is linear correlation, so the sum of the twist system can be given as

$$w_{\mathrm{p}}\boldsymbol{S}_{\mathrm{p}} + w_{\mathrm{P}_5}\boldsymbol{S}_{\mathrm{P}_5} + w_{\mathrm{P}_6}\boldsymbol{S}_{\mathrm{P}_6} + \sum_{i=9}^{12} w_{\mathrm{R}_i}\boldsymbol{S}_{\mathrm{R}_i} = 0 \tag{4}$$

where w_{p}, w_{P_5}, w_{P_6}, $w_{\mathrm{R}_i}\ (\mathrm{i} = 9,...,12)$ are linear correlation coefficient.

However, because the twists, $\boldsymbol{S}_{\mathrm{R}_9}$, $\boldsymbol{S}_{\mathrm{R}_{10}}$, and $\boldsymbol{S}_{\mathrm{R}_{11}}$ are always parallel and coplanar to each other in both deployment motion and grasping motion, so they are linear correlation and one conclusion can been drawn as

$$\sum_{i=9}^{12} w_{\mathrm{R}_i}\boldsymbol{S}_{\mathrm{R}_i} = 0 \tag{5}$$

Therefore, because the twists $\boldsymbol{S}_{\mathrm{P}_5}$ and $\boldsymbol{S}_{\mathrm{P}_6}$ are linear independence, we have $w_{\mathrm{p}} \neq 0$, there is no singularity in deployment motion of the module. Similarly, in grasping motion process of the module, only twist $\boldsymbol{S}_{\mathrm{p}}$ is replaced by twist, $\boldsymbol{S}_{\mathrm{R}} = (0,\ 1,\ 0;\ 0,\ 0,\ f_{\mathrm{R}_9})$. Apparently, $w_{\mathrm{R}} \neq 0$, so there is also no singularity in grasping motion of the module.

B. *Assembling of the Grasper*

In order to complete the assembly of the grasper, first, we need to study the connection of two adjacent modules. Unlike the traditional serial graspers, which always rigidly connect two adjacent modules, the proposed grasper is assembled by mobile connections of the modules. The key problem is that these basic modules are not rigid links but movable mechanisms, so two adjacent modules must be connected without influencing their motions. In addition, another significant requirement is that each module of grasper can be deployed synchronously. Detailed connection is as shown in Fig. 4.

Connecting mechanism is made up of a metamorphic mechanism, link 8_{C}, and link 9_{C}. Link 8_{C} is rigidly connected with metamorphic mechanism and link 9_{C}. Then, scissor-shaped mechanism of upper module is connected with connecting mechanism by revolute joint R_{C7} and R_{C8}. Link 11 of upper module is connected with connecting mechanism by revolute joint R_{C9}. Link 15 of upper module is connected with connecting mechanism by prismatic joint P_{C6}. Finally, scissor-shaped mechanism of lower module is connected with connecting mechanism by revolute joint R_{C5} and R_{C6}, link 10 of lower module is connected with connecting mechanism by revolute joint R_{C11}.

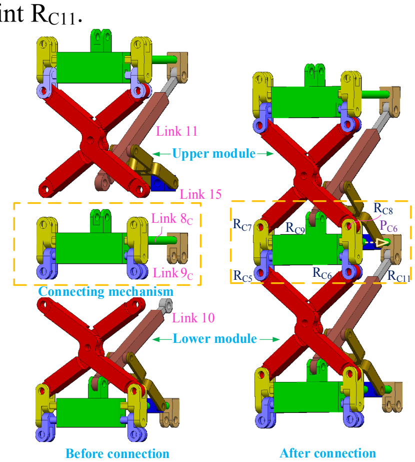

Fig. 4 Module connection.

Using this connecting method, the two adjacent modules can achieve coupled deployment mobility and independent grasping mobility.

In addition, to ensure that every module can be deployed to the middle of the grasper, a unique design is as shown in Fig. 5. Link 16 is connected with scissor-shaped mechanism of the first module by revolute joint R_{14} and base by prismatic joint P_7. In this way, a deployable robotic grasper composed of five modules could be assembled, the folded configuration and grasping configuration is as shown in Fig. 6.

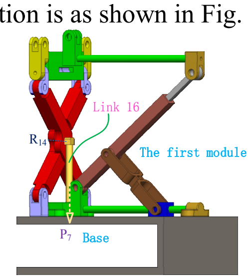

Fig. 5 Connection of base and the first module.

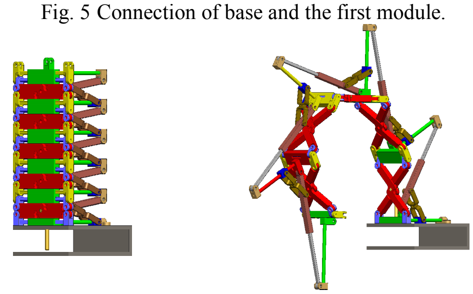

(a) Folded configuration. (b) Grasping configuration.

Fig. 6 The grasper with five metamorphic modules.

III. The Deploy/Fold Ratio Analysis

For large-scale unknown objects, one of the most important problems is how to transport and store the deployable robotic grasper, so a good deploy/fold ratio is required. The method to raise the deploy/fold ratio is presented. The folded configuration and deployed configuration of the module are as shown in Fig. 7.

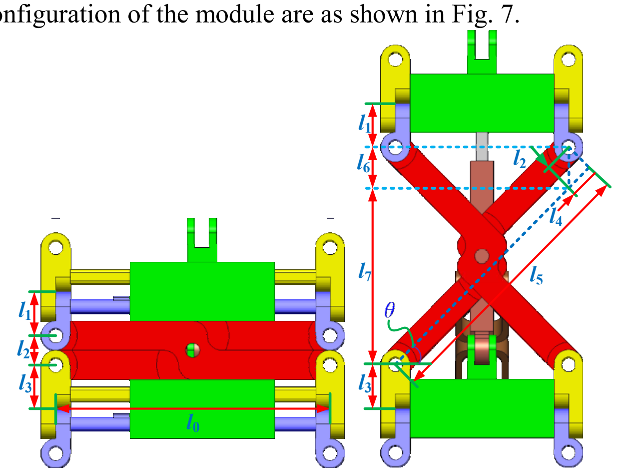

Fig. 7 Deploy/fold analyzed of the module.

The height of the folded configuration can be given as

$$H_1 = 2l_1 + l_2 + 2l_3 \tag{6}$$

where l_2 is the minimum height of scissor-shaped mechanism, l_1 and l_3 have been given as shown in Fig. 7.

Adding a module to the grasper increases the height of the grasper by $l_1 + l_2 + l_3$. Thus, the minimum height of the grasper consisting of n modules is

$$H_1^{'} = l_1 + l_3 + n(l_1 + l_2 + l_3) \tag{7}$$

In addition, the maximum height of the module is as shown in Fig. 7. Based on geometric relations, l_4, l_5, l_6, and l_7 can be determined by l_0, l_1, l_2, l_3, and θ ,which can be summarized as

$$\begin{cases} l_5 = l_0 \\ l_4 = l_2 \tan\theta \\ l_6 = \dfrac{l_2}{\cos\theta} \\ l_7 = (l_5 - l_4)\sin\theta \end{cases} \tag{8}$$

where l_4, l_5, l_6, and l_7 have been given in Fig. 7, θ is the angle between horizontal direction and scissor-shaped mechanism.

The maximum height of the module can be given as

$$H_2 = 2l_1 + 2l_3 + l_6 + l_7 \tag{9}$$

So if the grasper is made up of n modules, the maximum height of the grasper can be given as

$$H_2^{'} = l_1 + l_3 + n\left(l_1 + l_3 + l_6 + l_7\right) \tag{10}$$

Substitute (8) into (10), we have

$$H_2^{'} = l_1 + l_3 + n\left[l_1 + l_3 + \frac{l_2}{\cos\theta} + \left(l_0 - l_2\tan\theta\right)\sin\theta\right] \tag{11}$$

Based on the above analysis, the deploy/fold ratio ρ can be easily obtained of the grasper with n modules as

$$\rho = \frac{l_1 + l_3 + n\left[l_1 + l_3 + \dfrac{l_2}{\cos\theta} + \left(l_0 - l_2\tan\theta\right)\sin\theta\right]}{l_1 + l_3 + n(l_1 + l_2 + l_3)} \tag{12}$$

One conclusion can be drawn that the deploy/fold ratio ρ is mainly determined by the values of l_0, l_1, l_2, l_3, and θ, in which the values of l_1, l_2, and l_3 are always determined by stiffness condition of the proposed grasper. So if stiffness condition of the grasper is determined, the values of l_1, l_2, and l_3 are also decided. Thus, it is difficult to change the deploy/fold ratio by adjusting the values of l_1, l_2, and l_3.

However, the value of l_0 determines the length of scissor-shaped mechanism and the angle θ is the deployment angle of the scissor-shaped mechanism, which can be adjusted in design. With the increase of the angle θ and the value of l_1, the deploy/fold ratio will increases while the stiffness of the module will decreases. In this paper, the maximum of θ is 45° and the value of l_0 is 95mm. The real deploy/fold ratio of the finger is $\rho = 2.26$, which ensures that the DRG not only can be folded into a compact configuration but also have higher grasping stiffness.

IV. Workspace and Dexterity Analysis

To grasp objects with different shapes, a large reachable workspace is necessary in practice. The schematic diagram of the proposed grasper is as shown in Fig. 8. Then, a plane coordinate frame {*O-XY*} is set with *X*-axis towards the left of horizontal direction, *Y*-axis along to the up of vertical direction.

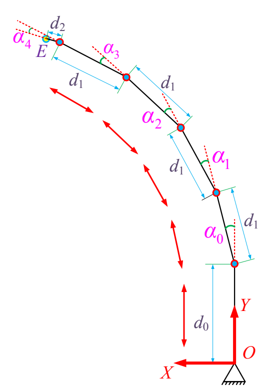

Fig. 8 Schematic diagram of the grasper.

Before the grasper carries out grasping motion, the modules are fully deployed, as shown in Fig. 9. Where the point *A* is the metamorphic position of module 1. Similarly, the point B_i, C_i, D_i, and E_i are the metamorphic positions of module 2, module 3, module 4, and module 5. The range of the grasping angle $\alpha_i (i = 0,...,4)$ is from 0° to 60°. Assume that $\alpha_i (i = 0,...,4) = 0$, the parameters of the arc scanned by the end-effector of the grasper are as shown in TABLE I. The workspace of the grasper is as shown in Fig. 9, which consists of ten areas. So the workspace of the grasper can be given as

$$S = S_1 + S_2 + S_3 + S_4 + S_5 + S_6 + S_7 + S_8 + S_9 + S_{10} \qquad (13)$$

It is clearly that the workspace of the grasper is quite large.

TABLE I
THE PARAMETERS OF THE ARC

Arc	Center	Radius	Central angle
G_1G_2	E_1	d_2	60°
G_1G_3	D_1	d_1+d_2	60°
G_1G_7	C_1	$2d_1+d_2$	60°
G_1G_{11}	B_1	$3d_1+d_2$	60°
G_1G_{16}	A	$4d_1+d_2$	60°
G_2G_4	D_1	D_1G_2	60°
G_3G_4	E_2	d_2	60°
G_3G_6	C_1	C_1G_3	60°
G_4G_5	C_1	C_1G_4	60°
G_5G_6	E_3	d_2	60°
G_5G_8	B_1	B_1G_5	60°
G_6G_7	D_2	d_1+d_2	60°
G_6G_9	B_1	B_1G_6	60°
G_7G_{10}	B_1	B_1G_7	60°
G_8G_9	E_4	d_2	60°
G_8G_{12}	A	AG_8	60°
G_9G_{10}	D_3	d_1+d_2	60°
G_9G_{13}	A	AG_9	60°
$G_{10}G_{11}$	C_2	$2d_1+d_2$	60°
$G_{10}G_{14}$	A	AG_{10}	60°
$G_{11}G_{15}$	A	AG_{11}	60°
$G_{12}G_{13}$	E_5	d_2	60°
$G_{13}G_{14}$	D_4	d_1+d_2	60°
$G_{14}G_{15}$	C_3	$2d_1+d_2$	60°
$G_{15}G_{16}$	B_2	$3d_1+d_2$	60°

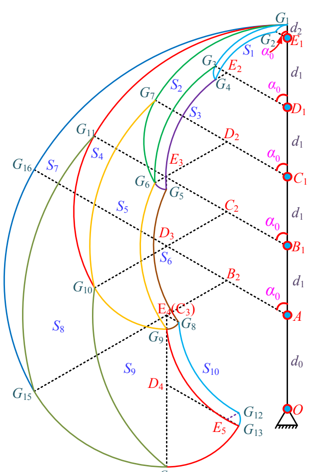

Fig. 9 Workspace of the grasper.

In addition, the dexterity of grasper is also significance because it determines the ability of the grasper position and orient the end-effector. To raise the dexterity, the approach presented in [14] is used in this paper. Such approach is to let the grasping angles of the modules to be same. Based on this approach, we let $\alpha_0 = \alpha_1 = \alpha_2 = \alpha_3 = \alpha_4 = \alpha$, and assume that the range of d_1 is $40\text{mm} \le d_1 \le 114\text{mm}$, then one can calculate the dexterity of the proposed grasper. As shown in Fig. 8, the position of the end-effector can be calculated by

$$\begin{cases} X_E = d_1\left[\sin\alpha + \sin(2\alpha) + \sin(3\alpha) + \sin(4\alpha)\right] + d_2\sin(5\alpha) \\ Y_E = d_0 + d_1\left[\cos\alpha + \cos(2\alpha) + \cos(3\alpha) + \cos(4\alpha)\right] + d_2\cos(5\alpha) \end{cases} \qquad (14)$$

where $E(X_E, Y_E)$ is the position of the end-effector, d_0 is the distance from bottom of base to the axis of the first metamorphic position, d_1 is the distance of the axis of two adjacent metamorphic positions, d_2 is the distance from end-effector to the axis of the last metamorphic position.

The derivative of (14) is

$$\begin{pmatrix} \dot{X}_E \\ \dot{Y}_E \end{pmatrix} = \boldsymbol{J}(d_1,\ \alpha)\begin{pmatrix} \dot{d}_1 \\ \dot{\alpha} \end{pmatrix} \qquad (15)$$

where $\boldsymbol{J}(d_1,\ \alpha)$ represents the Jacobian matrix of the grasper, which can be calculated by

$$\boldsymbol{J}(d_1,\ \alpha) = \begin{bmatrix} \dfrac{\partial X_E}{\partial d_1} & \dfrac{\partial X_E}{\partial \alpha} \\ \dfrac{\partial Y_E}{\partial d_1} & \dfrac{\partial Y_E}{\partial \alpha} \end{bmatrix} \qquad (16)$$

Now the dexterity measure w of the proposed grasper can be easily calculated as follows:

$$w = \sqrt{\det\left|\boldsymbol{J} \bullet \boldsymbol{J}^T\right|} \qquad (17)$$

The dexterity measure value of the grasper is as shown in Fig. 10. One can see that the dexterity of the proposed grasper increases as the length d_1 of the module increases.

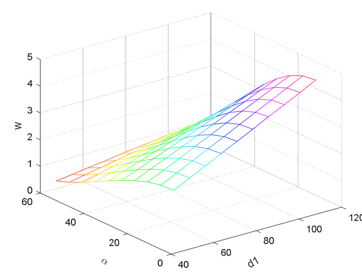

Fig. 10 The dexterity of the proposed grasper.

V. ANALYSIS OF SHAPE ADAPTABILITY

In this section, shape adaptability and grasping simulation are conducted. Generally, grasping pattern can be mainly divided into two categories: finger-tip grasp and enveloping grasp. Finger-tip grasp has been widely used in many serial graspers, which only uses one point of link to contact with objects. The most important advantage of this grasping pattern is that it is easily to realize dexterous manipulation. Compared to finger-tip grasping pattern, enveloping pattern is suitable for large-scale unknown objects because there exist multiple distributed contacting points. These contacting points will increase the stiffness of grasp especially for some large mass objects. As shown in Fig. 11, compared with two armed robot with simple hands, the proposed grasper has a compactly folded configuration and a large deployed configuration, a higher grasping stiffness is ensured by multiple distributed contacting points. The grasping simulation results shows that the grasper proposed has excellent grasping performances for different-shaped objects.

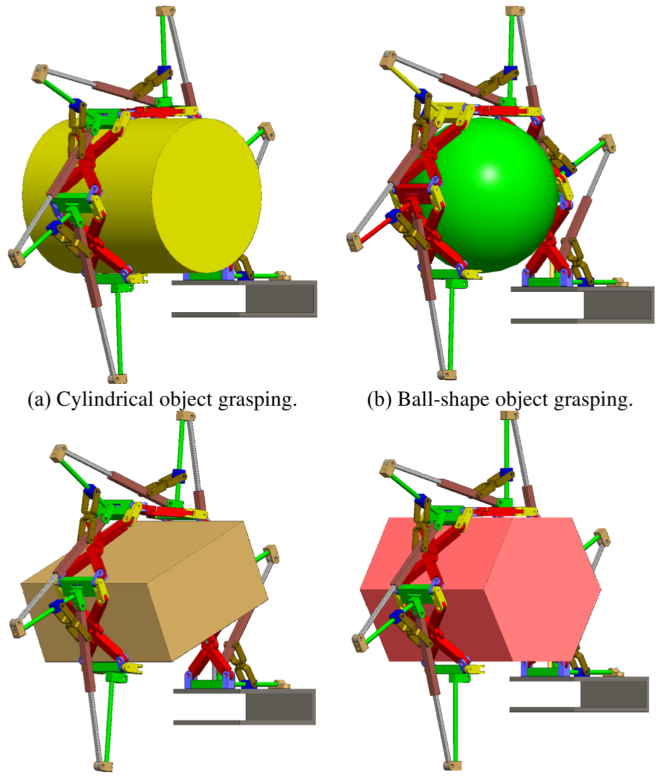

(a) Cylindrical object grasping. (b) Ball-shape object grasping. (c) Cuboid object grasping. (d) Hexagonal prism object grasping.

Fig. 11 Shape adaptability during the grasping motion.

VI. CONCLUSION

The paper proposed a novel deployable robotic grasper. A detailed mechanism design is introduced and metamorphic process is illustrated. Analysis shows that only single actuator can be used to drive the module to conduct both deployment motion and grasping motion. Then, by analysing the deploy/fold ratio and its influencing factors, the methods of calculating and raising deploy/fold ratio are proposed. Kinematic analysis illustrates the proposed grasper has a large reachable workspace. Finally, shape adaptability and grasping simulation prove that the deployable robotic grasper can be used to grasp large-scale unknown objects.

ACKNOWLEDGMENT

This work was financially supported in part by the national Science Foundation of China (Grant Nos. U1613201 and 51835002), in part by the Shenzhen Research Funds (Grant Nos. JCYJ20170413104438332, JCYJ20170811160940162), and in part by the Shenzhen Key Laboratory Fund of mechanisms and Control in Aerospace (Grant Nos. ZDSYS 201703031002066).

REFERENCES

[1] C. Li, X. Gu, and H. Ren, “A cable driven flexible robotic grasper with lego-like modular and reconfigurable joints,” *IEEE/ASME Transactions on Mechatronics*, Vol. 22, no. 6, pp.2757-2767, December 2017.

[2] O. Ryuta and T. Kenji. “Grasp and Dexterous Manipulation of Multi-Fingered Robotic Hands: A Review From a Control View Point,” *Advanced Robotics*, Vol. 31, pp. 1030-1050, October 2017.

[3] Q. C. Li, Z. Huang, and H. J.M, “Type synthesis of 3R2T 5-DOF parallel mechanisms using the Lie group of displacement,” *IEEE Transactions on Robotics and Automation*, vol. 20, no. 5, pp. 173-180, April 2004.

[4] C. Q. Gao, H. L. Huang, B. Li, and G. L. Jia, “Design of the truss-shaped deployable grasping mechanism using mobility bifurcation,” *Mechanism and machine Theory*, vol. 139, pp. 346-358, may 2019.

[5] R. L, “Design and Analysis of a Hybrid Serial-Parallel Manipulator,” *Mech. Mach. Theory*, vol. 34, no. 7, pp. 1037-1055, October 1999.

[6] B. Li, H. L. Huang, and Z. Q. Deng, “Mobility Analysis of Symmetric Deployable Mechanisms Involved in a Coplanar 2-Twist Screw System,” *Journal of Mechanisms and Robotics*, vol. 8, no. 1, p. 011007, February 2015.

[7] C. Shi, H. W. Guo, M. Li, R. Q. Liu, and Z. Q. Deng, “Type synthesis of deployable single-loop overconstrained linkages based on Bennett linkages,” *Mechanism and machine Theory*, vol. 120, pp. 1-29, February 2018.

[8] C. Shi, H. W. Guo, M. Li, R. Q. Liu, and Z. Q. Deng, “Conceptual configuration synthesis of line-foldable type quadrangular prismatic deployable unit based on graph theory,” *Mechanism and machine Theory*, vol. 121, pp. 563-582, March 2018.

[9] X. K. Song, Z. Q. Deng, H. W. Guo, R. Q. Liu, L. F. Li, and R. W. Liu, “Networking of Bennett linkages and its application on deployable parabolic cylindrical antenna,” *Mechanism and machine Theory*, vol. 109, pp. 95-125, March 2017.

[10] G. T. Li, H. L. Huang, H. W. Guo, and B. Li. “Design, analysis and control of a novel deployable grasping manipulator”, *Mechanism and machine Theory*, vol. 138, pp. 182-204, August 2019.

[11] J. S. Dai, Z. Huang, and L. Harvey, “Mobility of Over constrained Parallel Mechanism,” *Journal of Mechanical Design*, vol. 128, no. 1, pp. 220-229, October 2004.

[12] J. S. Dai and J. J. Rees, “Mobility in Metamorphic Mechanism of Foldable/Erectable Kinds,” *Journal of Mechanical Design*, vol. 121, no. 3, pp. 375-382, September 1999.

[13] L. Cui and J. S. Dai, “Reciprocity-Based Singular Value Decomposition for Inverse Kinematic Analysis of the Metamorphic Multi-fingered Hand,” *Journal of Mechanisms and Robotics*, vol. 4, no. 3, p. 034502, August 2012.

[14] S. Yahya, M. Moghavvemi, and H.A.F. Mohamed, “Geometrical approach of planar hyper-redundant manipulators: iiverse kinematics, path planning and workspace,” *Simulation Modelling Practice and Theroy*. vol. 19, no. 1, pp. 406-422. January 2011.